Iraqi Journal of Physics, 2024 *Vol. 22, No. 1, PP. 42-52*

https://doi.org/10.30723/ijp.v22i1.1175

P-ISSN: 2070-4003
E-ISSN: 2664-5548

Water Treatment Performance of PAN/HPMC/Gr Nano Composites

Masar A. Akaood[1a*], Iftikhar M. Ali[1b] and Basma I. Waisi[2c]
[1]*Department of Physics, College of Science, University of Baghdad, Baghdad, Iraq*
[2]*Department of Chemical Engineering, College of Engineering, University of Baghdad, Baghdad, Iraq*
[b]E-mail: iftali908@gmail.com, [c]E-mail: basmawaisi@coeng.uobaghdad.edu.iq
[a*]Corresponding author: masarabd8@gmail.com

Abstract

This study investigates polyacrylonitrile:hydroxypropyl methylcellulose (PAN:HPMC) and PAN:HPMC: graphene (Gr) composite nanofibers prepared using the electrospinning technique. Electrospinning is a simple and versatile technique that relies on the electrostatic repulsion between surface charges to continuously draw nanofibers from a viscoelastic fluid. Membrane technology is vital in removing contaminants due to its easy handling and high efficiency. The results demonstrated that the Gr was successfully incorporated into the PAN:HPMC nanofiber membranes, as confirmed by scanning electron microscopy, Fourier transform infrared spectroscopy (FTIR), and X-ray diffraction (XRD) measurements. The Gr content has a significant impact on the diameter, porosity, and pore size. The PAN:HPMC:0.02Gr electrospun nanofiber membranes achieved excellent oil rejection (72.47%) and good permeability flux (750 LMH); this might be a result of how well the functional groups of the equally distributed Gr within the PAN:HPMC nanofibers interacted with oil. It was noticed that oil rejection dropped a lot as the Gr content went up. This is likely because the pores got wider and some of the Gr stacked or agglomerated across the nanofibers.

Article Info.

Keywords:
Electrospinning, Polyacrylonitrile, Graphene, Nanocomposite, Water Treatment.

Article history:
Received: Jul. 27, 2023
Revised: Dec. 21, 2023
Accepted: Dec. 24, 2023
Published: Mar. 03,2024

1. Introduction

Nano-scale fibers made from polymers are being studied to offer cutting edge membranes for water treatment because of their large surface areas and flexible physical characteristics associated with filter structures, such as the size of pores and hydrophilicity [1-4]. The electrospinning method is cost-effective for creating continuous nano-scale threads from natural and man-made polymers. The electrospin nanofibers have outstanding characterizations such as a vast surface area-to-volume ratio, flexibility in surface functionalities, intrinsically high porosity, fully interconnected pore structures, low hydraulic resistance, and ease of scalable synthesis [5-7]. Finding the appropriate electrospinning settings without altering the materials' original structures is never easy because the overall physical properties of the produced materials are significantly impacted by the diameter/thickness of each nanofiber strand and/or the presence of additives [8-10].

Recently, nanofiber-based water treatment membranes have been produced by electro-spinning polyacrylonitrile (PAN) /hydroxypropyl methylcellulose (HPMC). It is often utilized as a pure substance in the fabrication of carbon-based fibers [11-14]. The porosity and size of pores of the resultant membranes can easily be modified by adjusting the electrospinning conditions, such as polymer concentration, solution viscosity, voltage, distance between needle nozzle and collector and flow rate [15-18]. However, the mechanical strength and chlorine resistance of PAN nanofiber membranes are often poor. To work around this limitation, PAN is typically hybridized with various polymers, inorganic, and carbon-based fillers [19-22].

Graphene (Gr) has drawn much attention among the many hybridizing supports since it is inexpensive and its composites enhance hydrophilicity, and chemical stability

while barely altering the fiber diameter and form [23-26]. Two-dimensional (2D) carbon-based material called Gr has a vast planar size and an atomic thickness [27-30]. Its distinctive structure provides high adsorption capacity, mechanical flexibility, and chemical stability due to the inclusion of functional groups like carboxylic, epoxy, and hydroxyl groups [31-34]. Gr may be dispersed uniformly throughout each PAN/ HPMC nanofiber thanks to electrospinning without affecting the fibers' natural structure. The loading of Gr into the PAN/HPMC nanofiber membranes enables careful investigation of their total physical properties. To determine the appropriate loading of Gr into synthetic membranes for water treatment applications, the rate of oil rejection and water flow (such as antifouling) were investigated [35-38].

This work aims to prepare PAN:HPMC and PAN:HPMC:Gr composite nanofiber membranes by the electrospinning method. This investigation encompasses a thorough analysis of the fabricated nanofiber membranes, which were characterized using X-ray diffraction (XRD) analysis, scanning electron microscopy (SEM), and the calculations of fiber size and porosity. The nanofiber membrane efficiency was applied in a cross-flow filtration system using emulsified kerosene in water.

2. Experimental Part

2.1. Materials

The materials used in this work are: PAN of average molecular weight Mw 150,000Da, HPMC, dimethy formamide (DMF) (≥ 99% and Mw of 73.10) and Gr nano powder (sky spring nanomaterial, Inc., USA). The emulsion solution was made using purified water and kerosene (from a midland Iraqi refinery firm).

2.2. Fabrication of the PAN/HPMC/Gr Composite Nanofiber Membranes

In this study, electrospinning was used to create the PAN:HPMC nanofibers through a series of steps. Initially, 1.55g of PAN was dissolved in DMF for two hours with continuous stirring until a homogeneous clear precursor solution was obtained. 1.05g of HPMC was dissolved in PAN:DMF using a magnetic stirrer for 4 hrs at room temperature. Following this, graphene powder of different concentrations (0.02, 0.04, 0.06, 0.08) wt% was introduced into the solution, which was stirred for 8 hrs at room temperature until it was completely dissolved. However, it is noteworthy to mention that adding graphene increased the viscosity of the resulting solution, necessitating an initial 30 min sonication to disperse the PAN:HPMC:Gr solutions effectively. Subsequently, these polymeric PAN: HPMC and PAN:HPMC:Gr solutions were loaded into a 5 mL plastic syringe equipped with a 22-gauge needle to act as a ground counter electrode, and an adjustable-speed metal drum was wrapped with aluminum foil. Then, for the next 8 hrs, electrospinning was carried with a tip-to-collector distance of 8 cm and 15kV. Table 1 provides definitions for the different samples indicated.

To create an oil-water emulsion, 1000 ml of distilled water and 1g of kerosene (97% pure, Fluka) were combined in a Hielscher ultrasonic processor (Hielscher UP400s, Teltow, Germany) at 10000 rpm for five min at room temperature, there was just (250 mg/L) of oil created. The amount of oil in the water was measured using a UV/Vis spectrophotometer (Thermo Scientific Genesys10S) operating at a (193nm) wavelength [39].

Table 1: The nanofiber membranes' preparation process.

PAN (g)	HPMC (g)	DMF (g)	Graphene wt%
1.55	1.05	17.4	0.02
1.55	1.05	17.4	0.04
1.55	1.05	17.4	0.06
1.55	1.05	17.4	0.08

2.3. Emulsified Oil Separation Experiments

The cross-flow filtration system shown in Fig. 1 was used for the tests concerning treating synthetic oily water. The setup included an unfinished cross-flow filtering cell, a feed pump, and a feed fluid tank. The flow and oil rejection rate of the manufactured PAN:HPMC based and PAN:HPMC:Gr nonwoven nanofiber membranes were examined under the same operating conditions. The manufactured electrospun nanofiber membranes (ENMs) were divided into (2x10) cm pieces and attached to membrane cells with an effective surface area of 20 cm^2. To start, the flux through the membrane was stabilized for the first 10 min by operating the filtering system with pure water. Next, an oil/water emulsion had to be filtered through the membrane for an hour. Baseline conditions included a temperature of 38°C, an oil concentration of 250 mg/L, and 60 ml/min of feed flow rate. To determine the contact angle of water drops with a contact angle analyzer (Theta Lite TL-101), the surface hydrophilicity of the manufactured ENMs membranes was investigated. The porosity of ENMs was computed using the gravimetric technique, this equation can be used to calculate porosity [40]:

$$\text{Porosity}(\varepsilon m) = \frac{(w_1 - w_2)}{A.t.\rho} \quad (\mathbf{1})$$

weights w_1 and w_2 refer to wet and dry membranes, respectively. A, t, and ρ are the membrane area, thickness, and water density at room temperature, respectively. Distilled water (as a wetting agent) was applied to the wet membrane samples (2x2cm) for five minutes. They were allowed to dry for five minutes at room temperature before weighing the membrane. The oil rejection percentage (R) (%) and membrane flow (litter per meter squared hour (L/m^2H) during a one-hour operation were calculated using Eqs.2 and 3, respectively [41]:

$$R\% = 1 - \frac{C_t}{C_\circ} * 100 \quad (\mathbf{2})$$

$$J = \frac{V}{A.t} \quad (\mathbf{3})$$

where: V is the permeate flow volume, Ais the membrane's effective surface area, and tis the filtering period. The oil concentrations in the feed and at any point during the experiment are C_0 and C_t, respectively.

2.4. Characterization of Nanofiber and Graphene Membranes

The FTIR spectra of graphene and the produced nanofiber membranes were acquired in the scan range 4000-400 cm^{-1} with a Tensor-27 FTIR analyzer (from Bruker Optics Inc., Billerica, Massachusetts). X-ray diffraction (XRD) patterns were measured using an X-ray diffractometer (HIMADZU 6000) to determine the intensity of the peaks as a function of Bragg's angle. Cu (k) at a wavelength of 1.5406 was the source of the

radiation. The scanning angle 2θ was changed between 10 and 40 degrees at a speed of 4 degrees per minute (these measurements were done at the Physics Department, College of Science, Al-Nahrain University). The PAN/HPMC/Gr nonwoven nanofiber membranes' surface morphology and structure were compared before and after oil removal with a field emission scanning electron microscope (FESEM, JEOL 6335F).

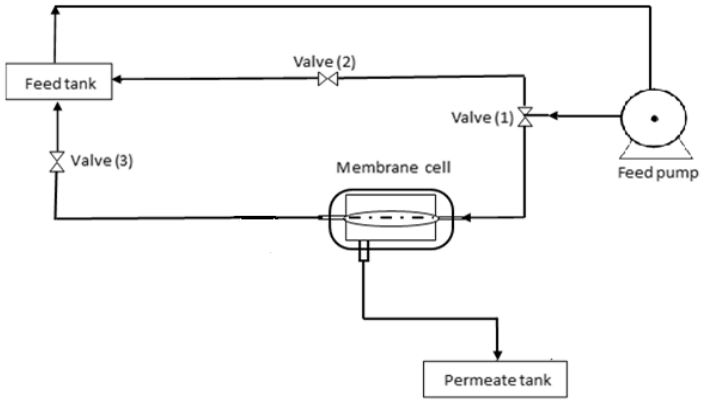

Figure 1: A schematic diagram of the system cross-flow filtration [2].

3. Results and Discussion

The crystalline structures of the nanocomposite PAN:HPMC and PAN:HPMC:Gr were examined using XRD measurements. The XRD patterns, shown in Fig. 2, showed that the overall structure of the synthesized nanofiber is consistent with the conventional polyacrylonitrile (PAN) structure. As a result, a distinctive diffraction peak for the structure was observed at a 2θ value of 17.1[42]. This peak is clear and strong and has a standard position at the phase (100). Two HPMC characteristic peaks were noted in the XRD pattern of the PAN/HPMC electrospun membrane at 2θ=14.3 and 2θ=21.8 suggesting that the lattice constant of the HPMC crystal has altered slightly. This shift may have been caused by drawing forces during the electrospinning process [43]. The XRD diffraction peaks in Fig. 3 of PAN:HPMC:Gr get sharper with increasing the graphene content. The graphene displayed a typical crystal form with characteristic peaks around 2θ=26.2, which corresponds to the (002); it was observed that the intensity of the characteristic peaks HPMC decreased, indicating that the material was in an amorphous state. In contrast, the diffraction peak intensities decreased in the PAN: HPMC. However, the original structure of PAN and cellulose was still visible in the composite, indicating good incorporation between the hybrid components [44].

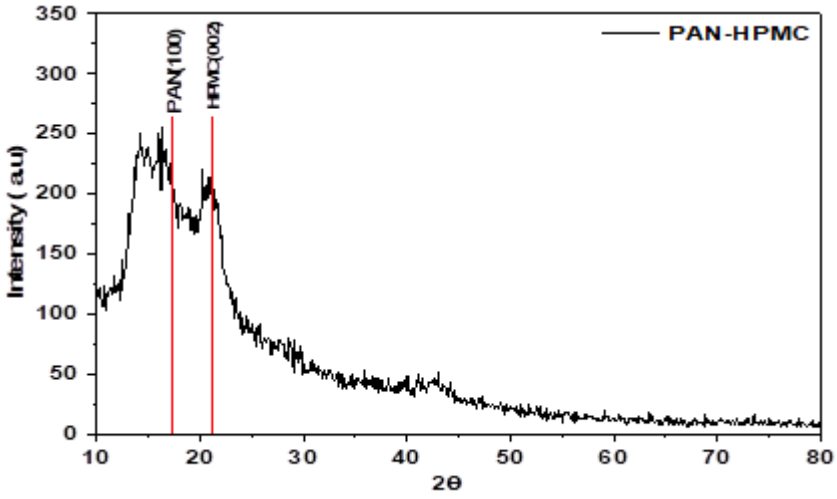

Figure 2: XRD pattern of PAN:HPMC nanofiber membrane.

FTIR spectra of the series PAN/HPMC and PAN/HPMC/G composite nanofiber membranes are shown in Figs. 4 and 5. PAN:HPMC and PAN:HPMC:Gr composite samples both showed characteristic peaks reflecting the stretching vibration of nitrile groups (C≡N) at 2242cm^{-1}. The peak at 3413cm^{-1} was associated with the stretching vibration of hydroxyl (O-H), while the stretching vibration of CH was indicated by the peak at 2918.47cm^{-1} [45]. On the membrane surface of PAN:HPMC:Gr, it was demonstrated that several active groups, including hydroxyl and carboxyl, were formed, which served as the foundation for the grafting reaction. The large peak between 1666.79 and 1739.49 cm^{-1} is caused by the stretching vibration of the (C=O) (ester bond). As a result of the C-H bending, the bandwidth from 497.452-745.86 cm^{-1} exists. The band (C=C) peak is centered at a wavelength of 1571.34 cm^{-1}, while the other peaks at 1375cm^{-1} are assigned to CH stretching aliphatic CH groups [46].

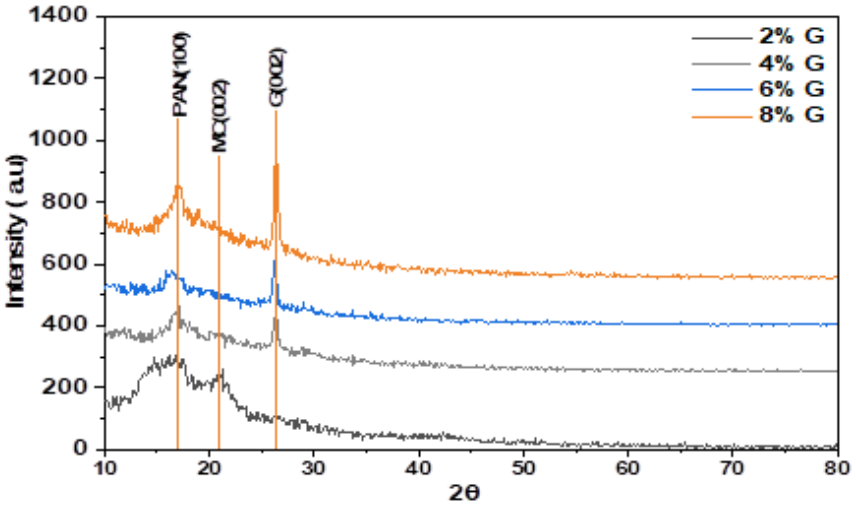

Figure 3: XRD pattern of PAN:HPMC:Gr nanocomposite film samples.

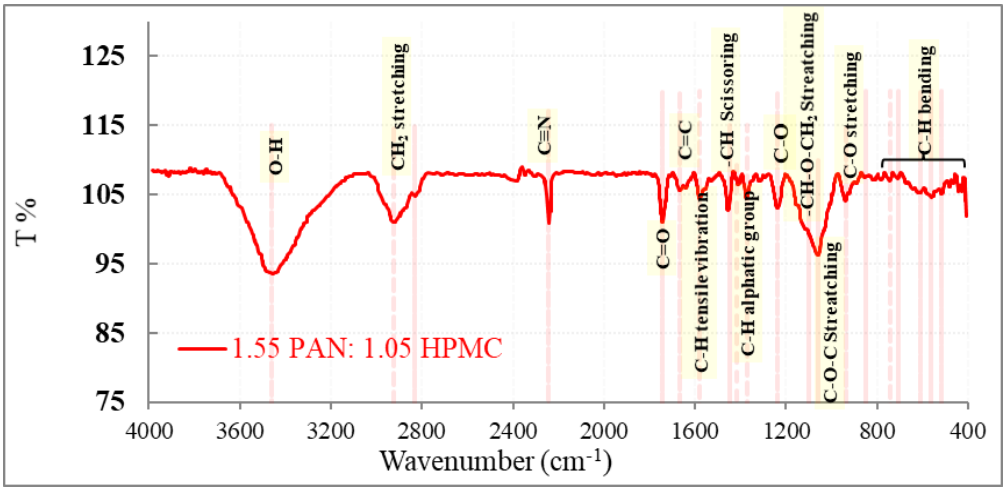

Figure 4: FTIR spectra of PAN:HPMC nanofiber membrane.

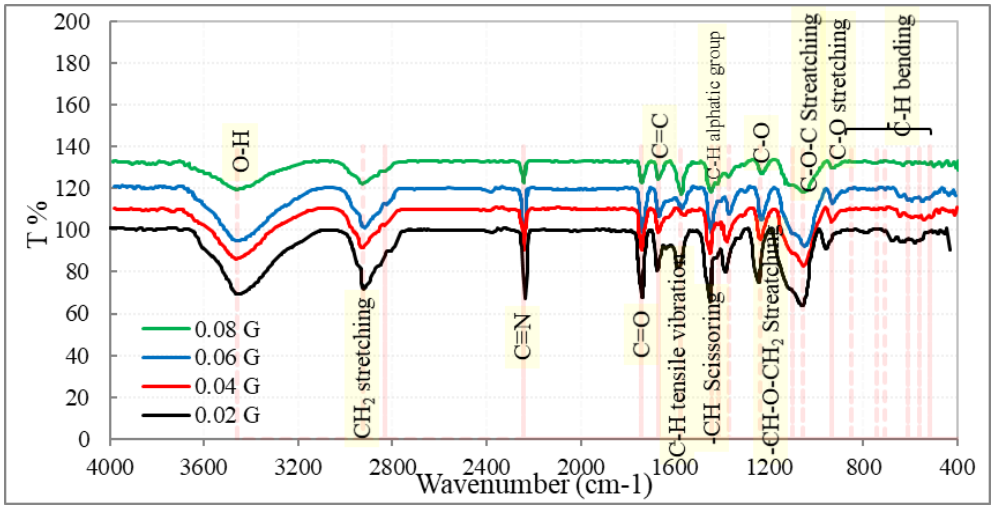

Figure 5: FTIR spectra of PAN:HPMC:Gr nanocomposite samples.

FESEM examination was performed to determine the membranes' general shape and the nanofibers' diameter, as shown in Fig. 6. According to top views, the packing of the nanofibers was remarkably consistent across all membranes. Comparatively to PAN:HPMC nanofibers, with the addition of graphene, the average diameter of the individual nanofiber strands and their distribution gradually grew. The composite nanofiber strands appeared somewhat rougher after adding graphene, and it was noticed that nodes began to appear on the nanofibers, indicating that the graphene was wrapped in the fibers, which has also been validated by other studies [47, 48].

FESEM images after oil filtration, shown in Fig. 7, clarified the formed fouling layer on the fabricated membranes. The fouling was the coalescence of oil droplets on the membrane surface during attempts at moving through the matrix. It can be noticed that the amount of fouling on the surface increased with decreasing the graphene concentration in the fabricated membrane because of the decrease of the fiber sizes that enhanced the excluding of the oil droplets on the membrane surface [49]. The porosity and the oil rejection percentage of PAN:HPMC and PAN:HPMC:Gr membranes were calculated and listed in Table 2.

Table 2: The general characteristics of PAN:HPMC and PAN:HPMC:Gr Composite Membranes.

Membrane	Ava. diameter (nm)	Porosity%	Rejection (R%)	flux(L/hm^2)
PAN/HPMC(60:40)	98	61.3	89	300
PAN/HPMC/0.02Gr	185	29.7	72.47	750
PAN/HPMC/0.04Gr	247	25.1	66.55	360
PAN/HPMC/0.06Gr	250	22.3	62.88	360
PAN/HPMC/0.08Gr	441	18.6	59.55	300

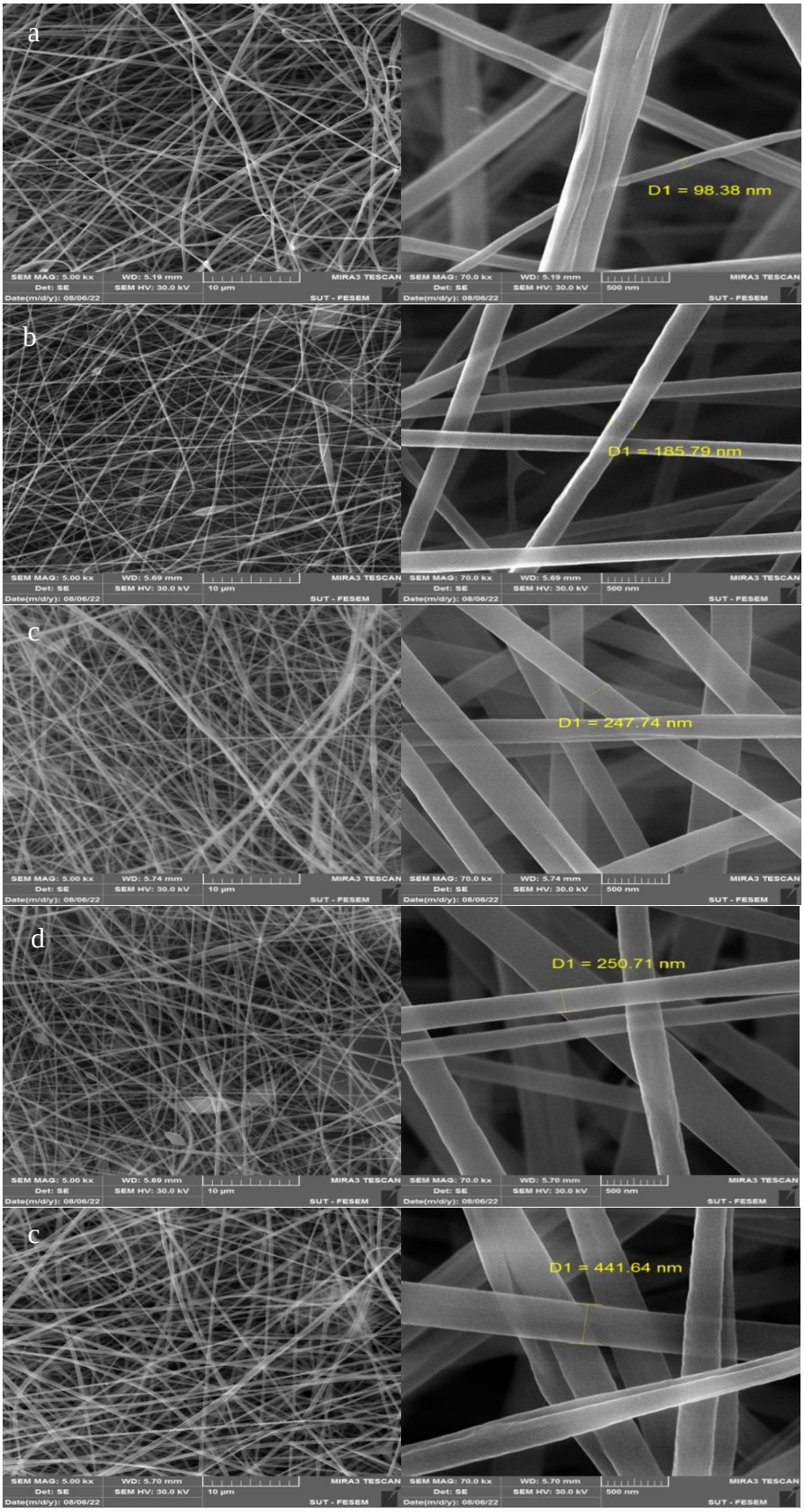

Figure 6: FESEM images of the nanofiber membranes (a) PAN:HPMC(60:40) (b) PAN:HPMC:0.02 wt % Gr, (c) PAN:HPMC:0.04 wt % Gr, (d) PAN:HPMC:0.06 wt %Gr, (e) PAN:HPMC:0.08 wt % Gr.

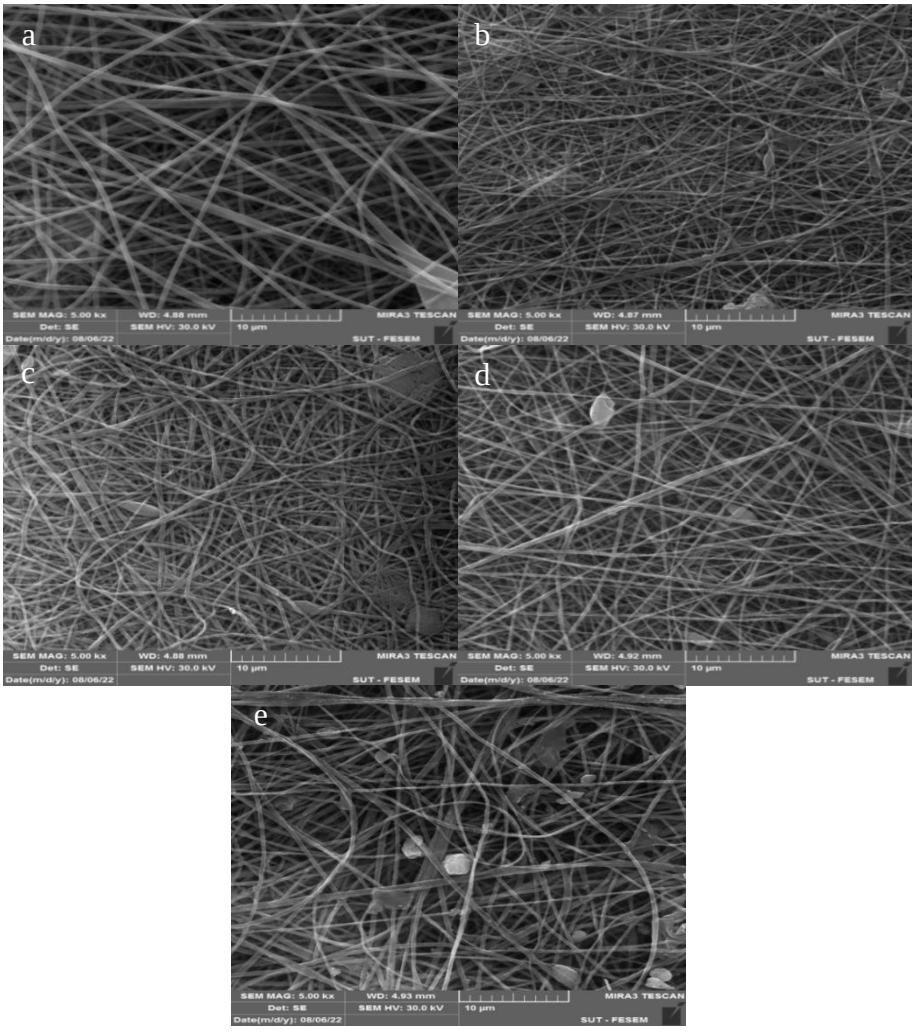

Figure 7: FESEM images of the different fabricated electrospun nanofibers membranes after oil filtration (a) PAN:HPMC (60:40) (b) PAN:HPMC:0.02 wt % Gr, (c) PAN:HPMC:0.04 wt % Gr, (d) PAN:HPMC:0.06 wt %Gr, (e) PAN:HPMC:0.08 wt % Gr.

Fig. 8 illustrates the performance (permeate flux and oil rejection percentage) of PAN:HPMC based membranes mixed with varying concentrations of graphene in emulsified oil filtration. Excellent permeability flux (750 L/hm^2) and good oil rejection (72.47%) were achieved by the PAN:HPMC:0.02wt%Gr membrane, which may have been due to the Gr's evenly distributed functional groups' effective interaction with oil in the PAN:HPMC nanofibers. It is evident that there has been a significant decrease in the rejection of oil, most likely as a result of the wider pore width and partial Gr aggregation/stacking across the nanofibers (i.e., the uneven distribution of graphene); this reduces the possibility of oil interacting with the embedded Gr's functional groups [50]. In general, the PAN:HPMC:Gr composite membranes showed efficient rejection of oil filtration.

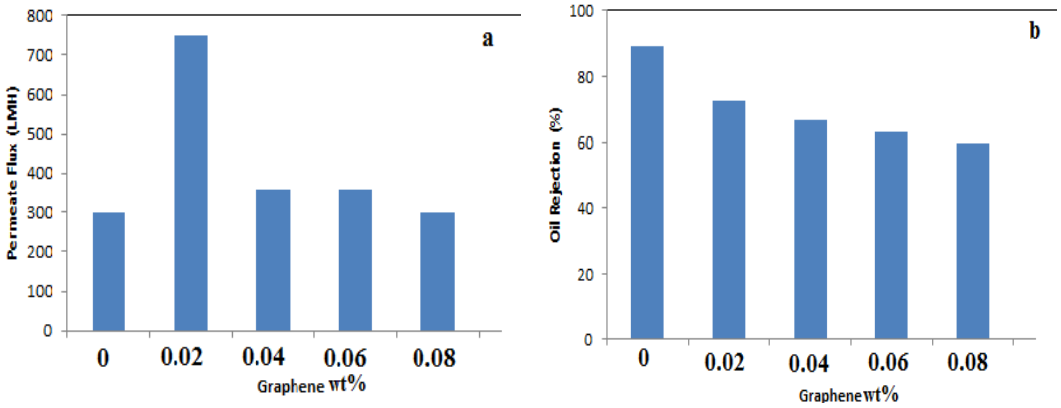

Figure 8: Efficiency of various manufactured membranes for oil/water filtration at oil concentration of 250 mg/L and temperature of 28°C (a) flux of permeate and (b)oil rejection.

4. Conclusions

This work effectively created ultrafine PAN:HPMC composite nanofibers with different Gr concentrations using the electrospinning technique. The XRD diffraction peaks of the PAN:HPMC:Gr become more sharp with increasing graphene content. The FESEM images of the membranes after oil filtration showed good oil rejection and an increase in water flow, due to the graphene containing hydrophilic function groups (hydroxyl and carboxyl groups), and the membranes become more hydrophilic. The membrane hydrophilicity reduces the oil fouling and enhances the water flux. In addition to increasing the concentration of graphene in the polymeric solution, it leads to an increase in viscosity composite, which in turn reduces the expansion of the flow of charge between the nanofibers, the growth in chain entanglement between polymer chains counteracts surface tension, culminating in the formation of thicker fibers and a decrease in the diameter of the membrane pores.

Acknowledgements

The authors would like to thank the University of Baghdad, College of Science, Department of Physics, and the thin film lab., many thanks are due to the Chemical Engineering Department, College of Engineering, Baghdad University for their continued efforts in completing the practical part of the study.

Conflict of Interest

The authors declare that they have no conflict of interest.

References

1. B. Barua and M. C. Saha, J. Appl. Poly. Sci. **132**, 41918 (2015).
2. H. S. Al-Okaidy and B. I. Waisi, Baghdad Sci. J. **20**, 1433 (2023).
3. Z. Zhao, J. Zheng, M. Wang, H. Zhang, and C. C. Han, J. Memb. Sci. **394**, 209 (2012).
4. H. M. Hawy and I. M. Ali, Optik **262**, 169263 (2022).
5. S. Faraji, M. F. Yardim, D. S. Can, and A. S. Sarac, J. Appl. Poly. Sci. **134**, 44381 (2017).
6. S. Alkarbouly and B. Waisi, Proceedings of 2nd International Multi-Disciplinary Conference (Sakarya, Turkey EAI, 2022). p.
7. J. Zhang, X. Pan, Q. Xue, D. He, L. Zhu, and Q. Guo, J. Membr. Sci. **532**, 38 (2017).
8. H. Yan, H. Wu, K. Li, Y. Wang, X. Tao, H. Yang, A. Li, and R. Cheng, ACS Appl. Mat. Inter. **7**, 6690 (2015).

9. A. A. Muhammad and I. M. Ibrahim, Neuro. Quant. **20**, 1984 (2022).
10. D. Chen, H. Feng, and J. Li, Chem. Rev. **112**, 6027 (2012).
11. H. M. Hawy and I. M. Ali, Optik **267**, 169659 (2022).
12. N. M. Aboamera, A. Mohamed, A. Salama, T. Osman, and A. Khattab, Mech. Advan. Mat. Struct. **26**, 765 (2019).
13. Y. Gao, J. Qin, Z. Wang, and S. W. Østerhus, J. Membr. Sci. **587**, 117136 (2019).
14. S. M. Alardhi, F. Y. Aljaberi, and L. M. Alsaedi, Egyptian J. Chem. **63**, 4963 (2020).
15. K. Venkatesh, G. Arthanareeswaran, A. C. Bose, P. S. Kumar, and J. Kweon, Sep. Purific. Tech. **257**, 117926 (2021).
16. H. Oliveira, A. Azevedo, R. Etchepare, and J. Rubio, Water Sci. Tech. **76**, 2710 (2017).
17. A. A. Abdel-Aty, Y. S. A. Aziz, R. M. Ahmed, I. M. Elsherbiny, S. Panglisch, M. Ulbricht, and A. S. Khalil, Sep. Purific. Tech. **253**, 117467 (2020).
18. M. Kadhom, K. Kalash, and M. Al-Furaiji, Chemosphere **290**, 133256 (2022).
19. M. S. Islam, A. N. Naz, M. N. Alam, A. K. Das, and J. H. Yeum, Coll. Inter. Sci. Commun. **35**, 100247 (2020).
20. J. C. Ge, G. Wu, S. K. Yoon, M. S. Kim, and N. J. Choi, Nanomaterials **11**, 2514 (2021).
21. I. Karbownik, O. Rac-Rumijowska, M. Fiedot-Toboła, T. Rybicki, and H. Teterycz, Materials **12**, 664 (2019).
22. S. Nithya, S. Selvasekarapandian, and M. Premalatha, Ionics **23**, 2767 (2017).
23. S. Huang, R. H. Ras, and X. Tian, Curr. Opin. Coll. Inter. Sci. **36**, 90 (2018).
24. M. L. Hassan, S. M. Fadel, R. E. Abouzeid, W. S. Abou Elseoud, E. A. Hassan, L. Berglund, and K. Oksman, Sci. Rep. **10**, 11278 (2020).
25. M. Shakiba, S. R. Nabavi, H. Emadi, and M. Faraji, Poly. Advan. Tech. **32**, 1301 (2021).
26. N. S. A. Rahman, M. F. Yhaya, B. Azahari, and W. R. Ismail, Cellulose **25**, 4887 (2018).
27. X. Wang, J. Yu, G. Sun, and B. Ding, Mat. Today **19**, 403 (2016).
28. M. Faccini, G. Borja, M. Boerrigter, D. M. Martín, S. M. Crespiera, S. Vázquez-Campos, L. Aubouy, and D. Amantia, J. Nanomat. **2015**, 2 (2015).
29. S. Liu, M. Kok, Y. Kim, J. L. Barton, F. R. Brushett, and J. Gostick, J. Electrochem. Soci. **164**, A2038 (2017).
30. W. Chen, Y. Su, L. Zheng, L. Wang, and Z. Jiang, J. Membr. Sci. **337**, 98 (2009).
31. Z. L. Kiss, S. Kertész, S. Beszédes, C. Hodúr, and Z. László, Desalin. Water Treat. **51**, 4914 (2013).
32. S. Ali, Z. Khatri, K. W. Oh, I.-S. Kim, and S. H. Kim, Macromol. Res. **22**, 562 (2014).
33. J. Fu, D. Li, G. Li, F. Huang, and Q. Wei, J. Electroanal. Chem. **738**, 92 (2015).
34. N. Hembach, J. Alexander, C. Hiller, A. Wieland, and T. Schwartz, Sci. Rep. **9**, 12843 (2019).
35. J. Lee, J. Yoon, J. H. Kim, T. Lee, and H. Byun, J. Appl. Poly. Sci. **135**, 45858 (2018).
36. C. Liao, X.-R. Zhao, X.-Y. Jiang, J. Teng, and J.-G. Yu, Microchem. J. **152**, 104288 (2020).
37. W. Jang, Y. Park, C. Park, Y. Seo, J.-H. Kim, J. Hou, and H. Byun, J. Membr. Sci. **598**, 117670 (2020).
38. N. Kumar and V. C. Srivastava, ACS Omega **3**, 10233 (2018).
39. M. A. Akaood, B. I. Waisi, and I. M. Ali, Iraqi J. Appl. Phys. **20**, 71 (2024).

40. M. Al-Furaiji, J. T. Arena, J. Ren, N. Benes, A. Nijmeijer, and J. R. Mccutcheon, Membranes **9**, 60 (2019).
41. Q. Wang, J. Cui, S. Liu, J. Gao, J. Lang, C. Li, and Y. Yan, J. Mat. Sci. **54**, 8332 (2019).
42. B. L. Abbood, K. A. Sukkar, and J. A. Al-Najar, J. Appl. Sci. Nanotech. **1**, 91 (2021).
43. A. H. Mohsan and N. A. Ali, Iraqi J. Phys. **20**, 14 (2022).
44. A. Almasian, M. Giahi, G. C. Fard, S. Dehdast, and L. Maleknia, Chem. Eng. J. **351**, 1166 (2018).
45. L. Deng, P. Li, K. Liu, X. Wang, and B. S. Hsiao, J. Mat. Chem. A **7**, 11282 (2019).
46. J. H. Li, H. Zhang, W. Zhang, and W. Liu, J. Biomat. Sci. Poly. Ed. **30**, 1620 (2019).
47. N. Naseeb, A. A. Mohammed, T. Laoui, and Z. Khan, Materials **12**, 212 (2019).
48. E. Mahmoudi, L. Y. Ng, W. L. Ang, Y. T. Chung, R. Rohani, and A. W. Mohammad, Sci. Rep. **9**, 1216 (2019).
49. Z.-Z. Yang, Q.-B. Zheng, H.-X. Qiu, J. Li, and J.-H. Yang, N. Carb. Mat. **30**, 41 (2015).
50. Z. Wang, A. Wu, L. Colombi Ciacchi, and G. Wei, Nanomaterials **8**, 65 (2018).

ادائية المتراكبات PAN/HPMC/Gr النانوية في معالجة المياه

مسار عبد كعود[1]، افتخار محمود علي[1]، بسمة اسماعيل ويسي[2]
[1] قسم الفيزياء، كلية العلوم، جامعة بغداد، بغداد, العراق
[2] قسم الهندسة الكيميائية، كلية الهندسة، جامعة بغداد، بغداد، العراق

الخلاصة

تبحث هذه الدراسة في الألياف النانوية المركبة PAN / HPMC / Gr التي تم تحضيرها باستخدام تقنية الغزل الكهربائي. الغزل الكهربائي هو تقنية بسيطة ومتعددة الاستخدامات تعتمد على التنافر الكهروستاتيكي بين الشحنات السطحية لسحب الألياف النانوية باستمرار من سائل لزج مطاطي، وتلعب تقنية الغشاء دورًا حيويًا في إزالة الملوثات نظرًا لسهولة التعامل معها وكفاءتها العالية. أظهرت النتائج أن المجهر الإلكتروني الماسح، والتحليل الطيفي للأشعة تحت الحمراء لتحويل فورييه، وقياسات XRD أكدت الإدماج الناجح لـ Gr في أغشية الألياف النانوية PAN / HPMC، التي يتأثر قطرها ومساميتها وحجم مسامها بشكل ملحوظ بكمية محتوى Gr. حقق غشاء PAN / HPMC/ 0.02Gr رفضًا ممتازًا للزيت (72.47٪) وتدفق جيد للنفاذية (LMH 750)؛ قد يكون هذا نتيجة لمدى تفاعل المجموعات الوظيفية من Gr الموزعة بالتساوي داخل ألياف نانوية PAN / HPMC مع الزيت. نلاحظ أنه مع زيادة محتوى Gr، انخفض رفض الزيت بشكل كبير، ويفترض أن ذلك يرجع إلى اتساع المسام وتجميع Gr جزئي أو متجمعة عبر الألياف النانوية.

الكلمات المفتاحية: الغزل الكهربائي، بولي أكريلونيتريل, الجرافين، المركب النانوي، معالجة المياه.